Plasma Science and Technology

PAPER

Experimental observation of reverse-sheared Alfvén eigenmodes (RSAEs) in ELMy H-mode plasma on the EAST tokamak

To cite this article: Tao ZHANG *et al* 2018 *Plasma Sci. Technol.* **20** 115101

View the article online for updates and enhancements.

This content was downloaded from IP address 210.73.19.208 on 06/09/2018 at 03:38

© 2018 Hefei Institutes of Physical Science, Chinese Academy of Sciences and IOP Publishing Printed in China and the UK

Plasma Sci. Technol. **20** (2018) 115101 (8pp) https://doi.org/10.1088/2058-6272/aac9b5

Experimental observation of reverse-sheared Alfvén eigenmodes (RSAEs) in ELMy H-mode plasma on the EAST tokamak

Tao ZHANG (张涛)[1], **Haiqing LIU** (刘海庆)[1], **Guoqiang LI** (李国强)[1], **Long ZENG** (曾龙)[1], **Yao YANG** (杨曜)[1], **Tingfeng MING** (明廷凤)[1], **Xiang GAO** (高翔)[1,2], **Hui LIAN** (连辉)[1], **Kai LI** (李凯)[1], **Yong LIU** (刘永)[1], **Yingying LI** (李颖颖)[1], **Tonghui SHI** (石同辉)[1], **Xiang HAN** (韩翔)[1] **and the EAST team**[1]

[1] Institute of Plasma Physics, Chinese Academy of Sciences, Hefei 230031, People's Republic of China
[2] University of Science and Technology of China, Hefei 230026, People's Republic of China

E-mail: hqliu@ipp.ac.cn

Received 13 March 2018, revised 31 May 2018
Accepted for publication 1 June 2018
Published 4 September 2018

Abstract

Reverse-sheared Alfvén eigenmodes (RSAEs) have been observed by using an interferometer and ECE diagnostics in NBI heated ELMy H-mode plasma on EAST tokamak. A typical feature of these modes is a fast frequency sweeping upward from ~80 kHz to ~110 kHz in hundred milliseconds during which the plasma temperature, density and rotation keeps no change. Only core channels of the interferometer can observe these modes, implying a core localized mode. The ECE measurement further showed that these modes located at about $\rho = 0.37$–0.46, just around the position of $q_{\min}$ with $\rho \sim 0.4$. These core localized modes are very weak in the magnetic fluctuations measured by mirnov probes mounted at the machine vacuum vessel. A multiple frequency fluctuation component, seemingly the so-called 'grand cascades', was also clearly observed on the ECE signal at $\rho = 0.46$. During the phase, a transient internal transport barrier (ITB) in ion temperature and toroidal rotation was observed and the ITB foot was just close to the position of $q_{\min}$. A modulation of RSAE frequency by ELM event was observed and this modulation could be attributed to rotation decrease or $q_{\min}$ increase due to ELM. Further study of these modes in EAST can provide valuable constraints for the q profile measurement and will be important for the long pulse operation.

Keywords: reverse-sheared Alfvén eigenmodes, ITB, q profile

(Some figures may appear in colour only in the online journal)

1. Introduction

Alfvén eigenmodes (AEs) are magnetohydrodynamic (MHD) instabilities destabilized by energetic particles in fusion devices [1, 2] and these modes could induce significant α particle losses in future fusion reactor [3]. Understanding and control of these instabilities will be important to realize self-sustained α particle heating in the reactors and they have been extensively studied in present devices [4]. One of these instabilities, reverse-sheared Alfvén eigenmodes (RSAEs) or Alfvén cascades (ACs), is well-known for its close relation to the reversed shear plasma and the internal transport barrier (ITB) [5]. The RSAEs have been used as a diagnostic to determine the safety factor (q) profiles in toroidal plasmas, i.e. so-called MHD spectroscopy [6, 7]. The RSAEs with fast frequency sweeping upward were firstly reported in the JT-60U tokamak [8, 9] and later observed in reverse sheared plasma of Alcator C-Mod [10] while the nature of those modes was not clear at that time. After the observation of RSAEs in JET [6], a theory has been developed to understand

the nature of these modes [11]. Based on the theory, the α particle driven modes observed in weak magnetic shear plasmas in TFTR D-T experiment, which were originally explained as toroidal Alfvén eigenmodes (TAEs), have been reinterpreted as RSAEs [12]. From then on, these modes have been observed in other devices, including DIII-D [13], NSTX [14], MAST [15], AUG [16] and LHD [17]. The RSAEs were also observed in sawtooth plasmas with the minimum value of q profile ($q_{\min}$) $\leqslant 1$ [18–20].

The RSAEs are shear-Alfvén eigenmodes associated with the extreme point of the Alfvén continuum localized at the magnetic surface of $q_{\min}$ in reversed shear plasma. The eigenfrequency of RSAEs can be expressed as [5]

$$\omega_{\mathrm{RSAE}}^2 = \omega_{\mathrm{G}}^2 + \frac{V_{\mathrm{A}}^2}{R^2}\left(n - \frac{m}{q_{\min}}\right)^2 + \omega_{\nabla}^2$$

$$\text{with } \omega_{\mathrm{G}}^2 = \frac{2}{m_{\mathrm{i}}R^2}\left(T_{\mathrm{e}} + \frac{7}{4}T_{\mathrm{i}}\right), \quad V_{\mathrm{A}} = \frac{B}{\sqrt{\mu_0 n_{\mathrm{i}} m_{\mathrm{i}}}} \tag{1}$$

where R is the major radius, m_{i} is the ion mass, T_{e} and T_{i} are electron and ion temperature respectively, B is the toroidal magnetic field, n_{i} is the ion density, ω_{G} is the geodesic acoustic frequency, V_{A} is the Alfvén velocity, m and n are poloidal and toroidal mode numbers repectively, ω_{∇} is an offset arising from plasma pressure gradient and fast-ion response and can be neglected in present experiments due to their small contributions. It can be seen from above formula that when $q_{\min}$ changes with time, the RSAEs frequency will change at a rate [21]

$$\frac{\mathrm{d}\omega_{\mathrm{RSAE}}}{\mathrm{d}t} \approx m\frac{V_{\mathrm{A}}}{R}\frac{\mathrm{d}}{\mathrm{d}t}q_{\min}^{-1} \tag{2}$$

so that the slope of mode frequency sweeping depends on the evolution of $q_{\min}$ and the mode with higher mode number has a higher sweeping rate. It can be further observed from equation (1) that RSAEs with all toroidal mode numbers, i.e. $n = 1, 2, 3\ldots$, can be present when $q_{\min}$ pass through an integer value. This so-called grand cascade phenomenon has been observed in experiment and used to accurately determine the appearing time of integer $q_{\min}$ [21, 22]. Numerous experiments have demonstrated a close link between the formation of ITB and the low order rational values of $q_{\min}$, particularly integer $q_{\min}$ [23–27]. This link has been used to develop ITB scenarios by inferring the integer $q_{\min}$ from the grand cascades on JET [21, 28].

In this paper, we will present the first experimental observation of RSAEs on the EAST tokamak. These modes were occasionally observed in the plasmas for developing long pulse high β_{N} operation [29]. The internal measurement from the interferometer and ECE diagnostics determined the mode location at $\rho = 0.37$–0.46, which is consistent with the position of $q_{\min}$, $\rho \sim 0.4$. A multiple frequency fluctuation component, seemingly the so-called 'grand cascades', was also observed and simultaneously a transient ion ITB was formed. For the rest of this paper, the experimental setup is described in section 2. Section 3 presents the experimental results. Finally, the results are summarized in section 4 and an outlook for future study will also be given.

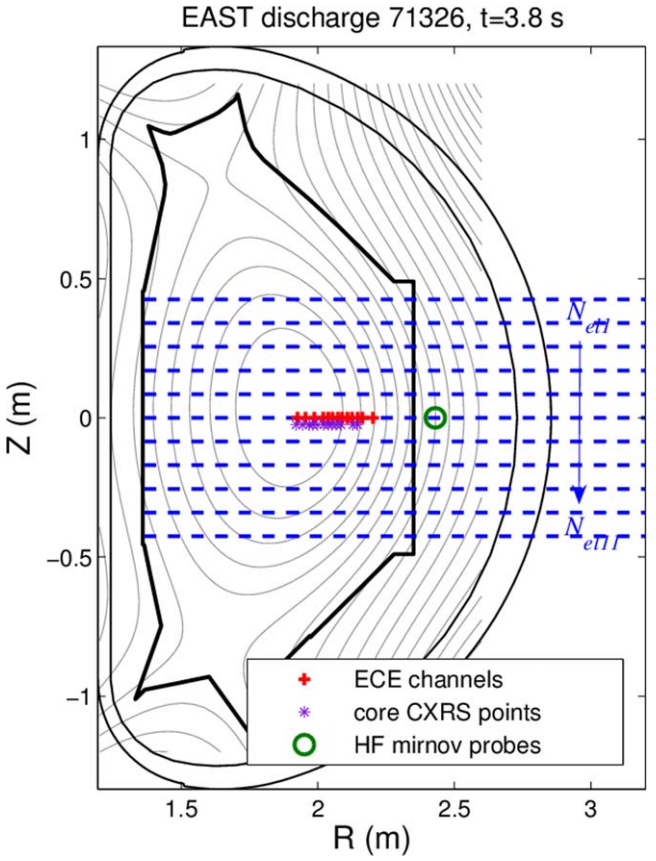

Figure 1. Poloidal view of diagnostics.

2. Experimental setup

The EAST is a fully superconducting tokamak with major radius $R_0 = 1.85$ m and minor radius $a = 0.45$ m, equipped with a molybdenum first wall, a graphite lower divertor and a ITER-like W/Cu upper divertor. The analyzed plasmas are for developing long pulse high β_{N} operation [29]. The auxiliary heating method in these plasmas is lower hybrid wave (LHW) at 4.6 GHz [30] and neutral beam injection (NBI) [31]. The NBI system is composed of two beam lines. One is injected in the co-current direction and another one is in the counter-current injection. For each beam line, there are two ion sources. The NBI power in the experiment is increased stepwise by setting the injection time of ion sources. The plasma current (I_{p}) is 450 kA and the toroidal magnetic field (B_{T}) is 1.6 T with an upper single null divertor configuration.

Figure 1 shows the poloidal view of the main diagnostics for analysis. POINT (POLarimeter-INTerferometer) diagnostics [32] were used to measure the line integrated densities and Faraday rotation angles. As shown in figure 1, POINT diagnostics have 11 channels and these channels are uniformly distributed along the vertical direction in the same poloidal cross-section. The vertical distance between adjacent beams is 8.5 cm. In this paper, the measured line integrated densities by POINT will be named from N_{el1} to N_{el11}. The line integrated density fluctuations can also be analyzed by performing the regular fluctuation analysis methods on these signals. In the experiment, the sampling frequency of POINT

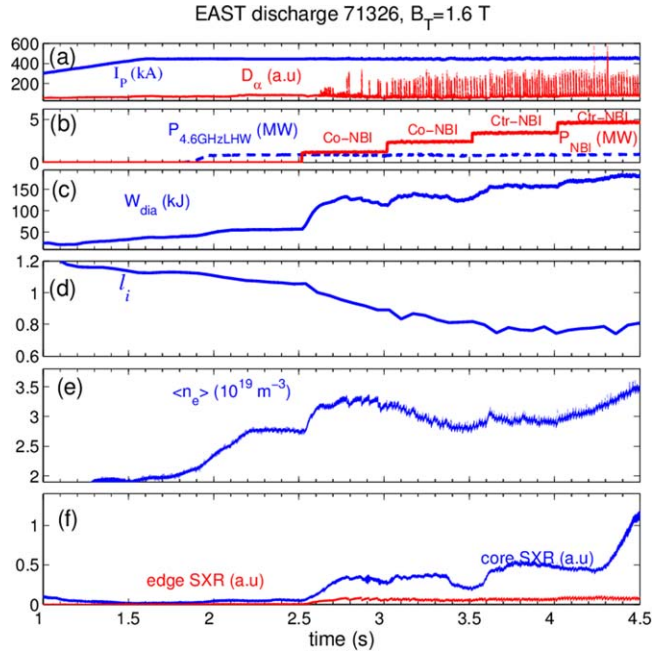

Figure 2. EAST discharge #71326 (a) plasma current (I_p) and D_α signal, (b) 4.6 GHz lower hybrid wave and NBI power steps, (c) plasma diamagnetic energy W_{dia}, (d) plasma inductance l_i, (e) plasma line averaged density $\langle n_e \rangle$ and (f) core and edge soft x-ray (SXR).

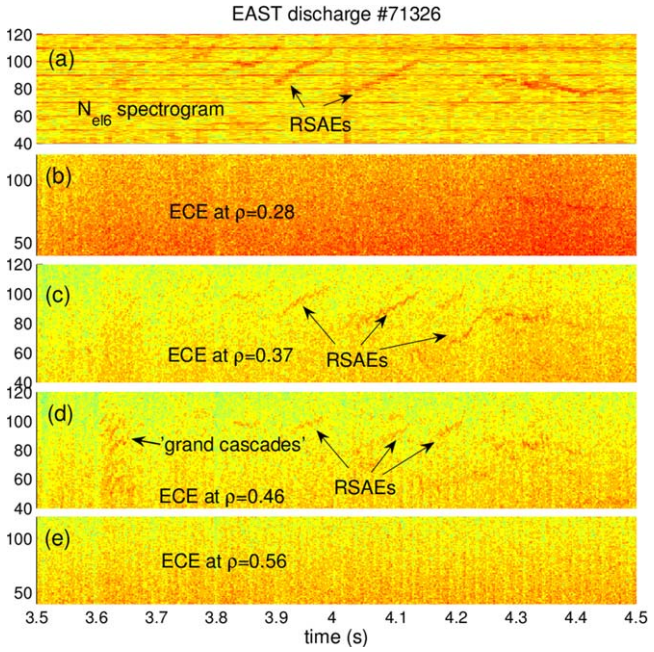

Figure 3. Spectrogram of fluctuation signals measured by (a) middle plane interferometer and (b)–(e) ECE channels at different radial positions.

diagnostics is 250 kHz and therefore the fluctuation mode with frequency up to 125 kHz can be measured. The current profile and thus q profile can also be obtained by using the measured Faraday rotation angles as additional constraints in EFIT equilibrium reconstruction [33]. A multichannel electron cyclotron emission (ECE) diagnostics [34] located in the midplane of low field side was used to measure electron temperature and temperature fluctuations. The fluctuation measurement used in this paper are mainly provided by the above two diagnostics. Due to the finite beam radius (w) of the two diagnostics in the poloidal direction, these diagnostics can only respond to the fluctuation with finite polodial wavenumbers, as presented in the appendix. In the experiment, the beam radii for the POINT and ECE diagnostics are about 1.4 cm and 4 cm respectively. According to the formula (A.4) in the appendix, therefore, the measurable fluctuations for the two diagnostics are with $k_\theta \leqslant 1.43\,\mathrm{cm}^{-1}$ and $k_\theta \leqslant 0.5\,\mathrm{cm}^{-1}$ respectively. Charge exchange recombination spectroscopy (CXRS) diagnostics were used to measure the core ion temperature and toroidal rotation profiles [35]. The magnetic fluctuations were measured by high frequency (HF) mirnov probes mounted on the vacuum vessel wall.

3. Experimental results

Figure 2 shows typical target plasma (EAST #71326). The plasma current is ramped up to 450 kA from $t = 0$ s to $t = 1.6$ s. A 1 MW 4.6 GHz LHW is injected in the plasma at $t = 1.8$ s and kept constant in the whole discharge. The NBI is applied at $t = 2.515$ s and then increases step by step. For the discharge shown in figure 2, the first two steps with power increased from 1.2 MW to 2.4 MW are from the co-current beam and the latter two steps (1 and 1.2 MW, respectively) are from the counter-current beam. The injected deuterium beam energies are 61 keV, 60 keV, 57 keV and 60 keV respectively for the four ion sources. The injected beam ion is sub-Alfvénic, $V_b/V_A = 0.55$ and the sideband resonance is therefore satisfied [2]. The plasma accessed H-mode at about $t = 2.53$ s.

A series of modes with fast frequency sweeping upward were firstly observed in the fluctuation spectrogram of line integrated density measured by POINT mid-plane channel (N_{el6}), as shown in figure 3(a). It will be shown later that these modes can be confirmed as RSAEs. It is further found that two adjacent ECE channels at $\rho = 0.37$ and $\rho = 0.46$ clearly pick up these modes while for the channels more inside or outside can not observe them. This means that these modes localize in the region $\rho = 0.37$–0.46. In addition, multiple frequency fluctuation components, seemingly the so-called 'grand cascades', was also clearly observed on ECE signal at $\rho = 0.46$ from 3.6 s to 3.7 s. It will be further discussed in the later paragraph. We have checked all the available fluctuation signals on EAST and found only several signals can pick up these modes. These signals include the three POINT channels around mid-plane, i.e. N_{el5}, N_{el6} and N_{el7}, and two ECE channels at $\rho = 0.37$ and $\rho = 0.46$ and high frequency (HF) mirnov probes mounted in the vacuum vessel wall. The fluctuation spectrograms of former five signals have been shown in figures 4(a)–(e). For magnetic fluctuation measured by mirnov probes, the RSAEs are very weak and cannot be easily distinguished from the auto-power spectrum. Nevertheless, the coherence spectrum between the magnetic fluctuation and ECE at $\rho = 0.37$ still can distinguish two bands of the RSAEs and is shown in figure 4(f). Due to very weak

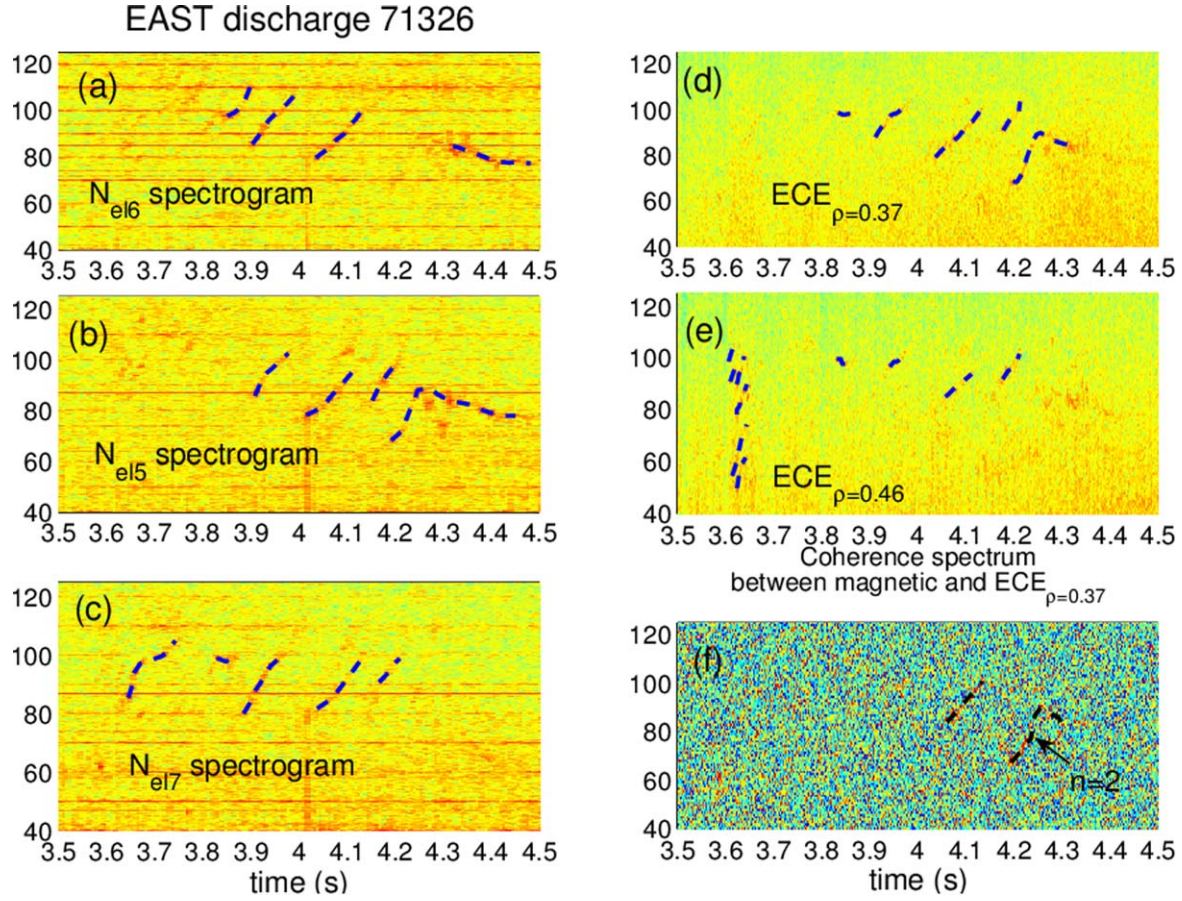

Figure 4. Spectrogram of the three middle channels of interferometers (POINT) in (a)–(c), ECE channels at $\rho = 0.37$ and $\rho = 0.46$ in (d)–(e) and (f) the coherence spectrum between the signals of edge magnetic probe and ECE at $\rho = 0.37$. The RSAEs frequencies have been indicated by dashed lines.

signals picked by mirnov probes, it is difficult to determine the toroidal mode numbers for these modes. The time evolutions of RSAEs mode frequencies can be directly extracted from each plot and have been over-plotted with dashed lines in figure 4. It can be seen that the bands of RSAEs picked up by different signals are not fully the same due to the different line-of-sights or different diagnostics instrument responses.

In order to demonstrate the complete picture of the RSAEs in the discharge, the time evolutions of each RSAEs band picked up by different signals in figure 4 have been combined together and shown in figure 5(a). It shows that the identical band measured by different diagnostics overlapped very well. For the band during the phase $t = 3.88$ s to 4.0 s, the mode frequency increased from 80 kHz to 103 kHz even though the plasma temperature, density and stored energy, shown in figure 5, keeps no change. This observation excludes the possibility that the frequency sweeping is due to the change of kinetic profile. Another well-known factor for the frequency sweeping of core mode is the toroidal rotation. This possibility can be also excluded as explained as follows. It can be observed from figure 5 that the change of the toroidal rotation velocity (ΔV_t) is not more than 10 km s^{-1} by considering the errorbar. If the frequency change (Δf) of the mode is due to the toroidal rotation change, then $\Delta f = n\Delta V_t/(2\pi R)$. For present discussed case, $\Delta f = 23$ kHz, $R = 1.85$ m, $\Delta V_t \leqslant 10$ km s^{-1}, the toroidal mode number n should be larger than 27. As discussed below, a mode with this large toroidal mode number can not be detected by our diagnostics. A tokamak plasma with helical magnetic field, parallel wave number ($k_{//}$), local poloidal wave number (k_θ) and toroidal mode number has the following relation

$$k_{//} = k_\theta \sin\alpha - k_\phi \cos\alpha = k_\theta \sin\alpha - \frac{n}{R}\cos\alpha \qquad (3)$$

where α is the local magnetic field pitch angle. So

$$k_\theta = \frac{n}{R}\frac{\cos\alpha}{\sin\alpha} + \frac{k_{//}}{\sin\alpha}. \qquad (4)$$

For a flute-like mode, $k_{//} \sim 0$ and the mode with finite $k_{//}$, e.g. TAEs, $k_{//} = n/2\mathrm{R}$ [2], the poloidal distributions of k_θ for the two kinds of mode with $n = 27$ have been shown in figure 6. The poloidal distribution of magnetic field pitch angle at $\rho = 0.4$ (position of $q_{\min}$) shown in figure 6(a) was calculated based on the EFIT reconstructed equilibrium. The pitch angle at low field side (LFS) is larger than that at high field side (HFS), which is a typical feature in tokamak device [36]. As a result, the k_θ takes a lowest value in LFS as shown in figure 6(b). This kind of poloidal distribution of k_θ is very similar to that calculated by NOVA-K code for RSAEs in DIII-D [37]. From figure 6, we can conclude that the lowest k_θ for $n = 27$ mode for present analyzed plasma is about

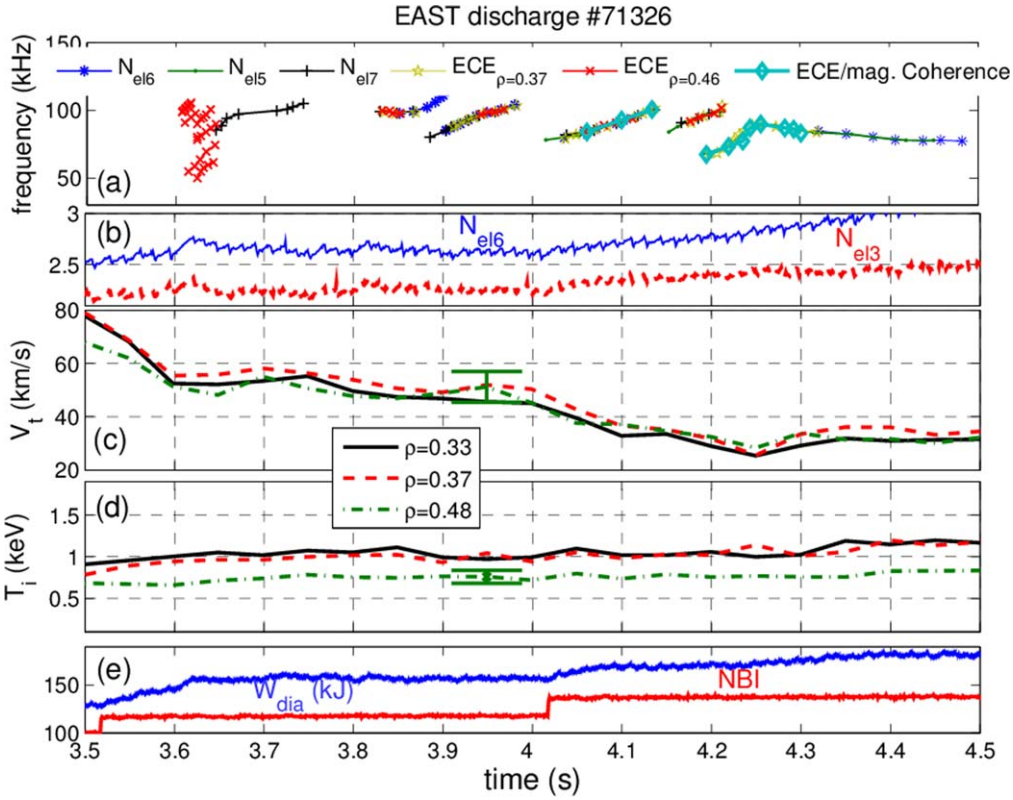

Figure 5. (a) The combined frequency behavior of RSAEs from figure 4, (b) the N_{el6} and N_{el3}, (c) and (d) the toroidal rotation velocity (V_t) and ion temperature (T_i) at three radial locations $\rho = 0.33$, $\rho = 0.37$ and $\rho = 0.48$. Typical errorbars for the two quantities are also plotted. (e) W_{dia} and NBI power step.

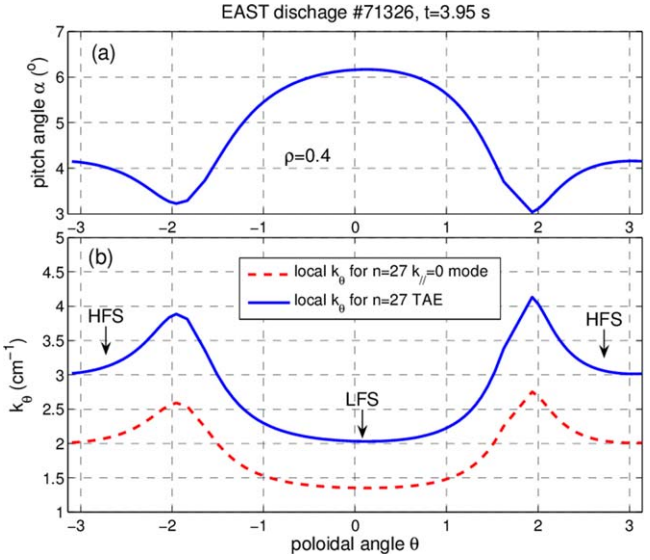

Figure 6. (a) The poloidal distribution of local magnetic pitch angle (α) at $\rho = 0.4$ for #71326, $t = 3.95$ s, (b) the poloidal distribution of local k_θ for $n = 27$ $k_{//} = 0$ mode and TAE mode calculated by using the formula (4) in the text.

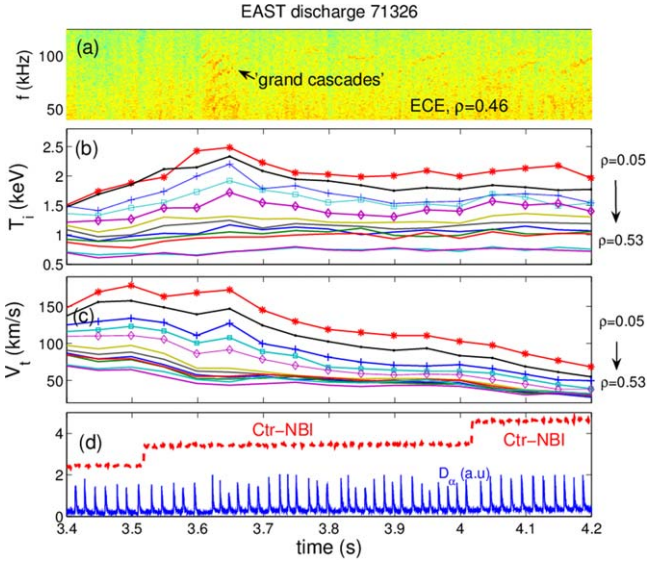

Figure 7. (a) Spectrogram of ECE channel at $\rho = 0.46$, (b) and (c) the time evolutions of T_i and V_t at different radial positions, (d) NBI power and D_α signal.

1.35 cm^{-1}, which is close to the upper limit of the POINT diagnostics k_θ resolution ($k_\theta \leqslant 1.43\,cm^{-1}$) but much exceeding that of the ECE diagnostics ($k_\theta \leqslant 0.5\,cm^{-1}$). That is to say, if the mode frequency sweeping from 3.88 s to 4.0 s in figure 5(a) is due to toroidal rotation change, the mode number should be larger than 27, which can not be measured by ECE diagnostics since the $n = 27$ mode poloidal k_θ is much beyond this diagnostics response. This clearly contradicted to the observation. Therefore, the mode frequency

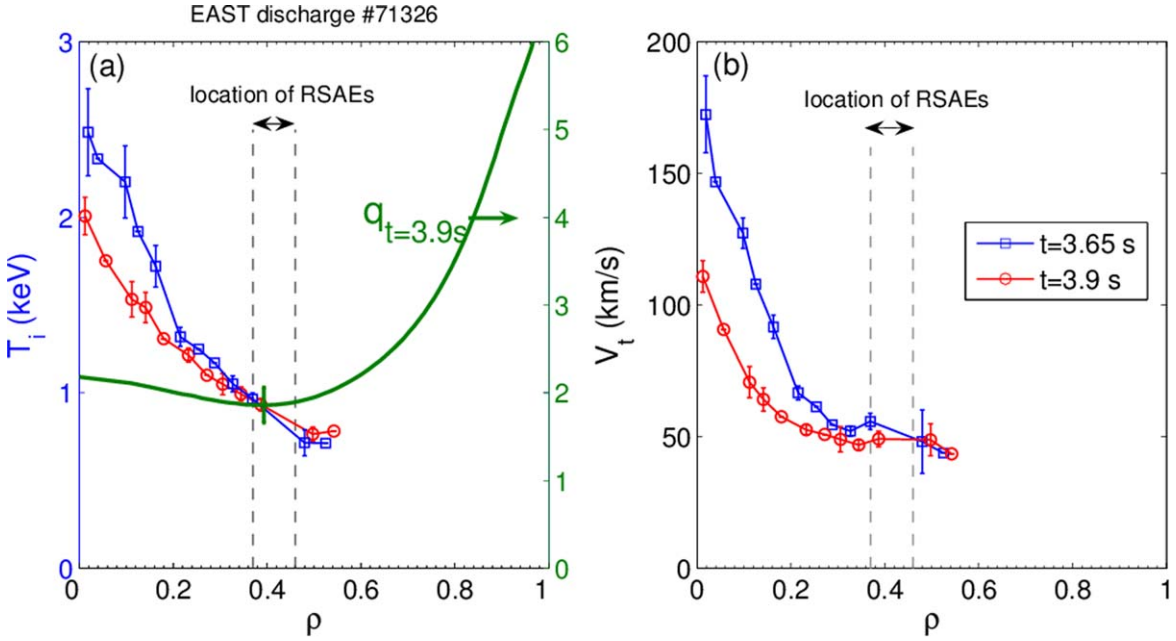

Figure 8. (a) The T_i profiles at $t = 3.65$ s and $t = 3.9$ s and q profile at $t = 3.9$ s and (b) V_t profiles. The vertical dashed lines indicated the radial locations of the RSAEs.

sweeping should be not due to the rotation change. From the above discussion, the observed mode frequency sweeping cannot be explained by the change of kinetic profile and also by the change of toroidal rotation. To our knowledge, only RSAEs could explain this observed frequency sweeping.

As shown in figure 3(d), the ECE spectrum at $\rho = 0.46$ demonstrates multiple frequency fluctuation components with frequency sweeping upward at about from 3.6 s to 3.65 s. These fluctuation components are very like the so-called 'grand cascades'. However, no determination of toroidal mode number for these modes precludes the final conclusion. Nevertheless, transient ion ITB was actually observed when these modes appeared, as shown in figure 7. The first counter NBI was applied at about 3.5 s and the core ion temperature (T_i) gradually increased and the V_t decreased. Here, positive V_t represented the plasma rotates in co-I_p direction and the V_t decreases was due to the counter rotation driven by the ctr-beam. However, the T_i experienced an abrupt increase from 3.6 s to 3.65 s and especially the V_t experienced a short time increase, implying an co-I_p rotation driven by some mechanisms. After that, both T_i and V_t in the core region gradually decayed and finally saturated up to the application of the second ctr-NBI at about 4.05 s. The abrupt increase of core T_i at 3.6 s to 3.65 s indicated the ITB formation in ion channel. Figure 8 shows the T_i and V_t profiles at 3.65 s and 3.9 s. It was found that the increase of T_i and V_t is mainly at $\rho \leqslant 0.4$, which could be considered as the ITB foot. The q profile at $t = 3.9$ s, obtained by using the Faraday rotation angles as additional constraints in EFIT equilibrium reconstruction, and the radial location of RSAEs were also shown for comparison. It can be observed that the q_{min} position was at about $\rho = 0.4$ and the RSAEs just located around the q_{min} position. This specific example showed that the q_{min} position is consistent with the ion ITB foot. The further discussion on the relation between the q_{min} position and ion ITB foot on EAST is beyond the scope of the present work and will be left for future study.

Lastly, we will show that RSAE frequency is modulated by ELM. Figure 9(a) shows that RSAE frequency (f_{RSAE}) on ECE spectrogram shows a decrease during each ELM event while general trend of f_{RSAE} presents sweeping upwards. The time evolution of f_{RSAE} is shown in figure 9(b). In this plot, f_{RSAE} and associated errorbar are determined by fitting the ECE power spectrum using a function $P = a \times \exp[-(f - f_0)^2/\Delta f^2] + b$, as shown in figure 9(e) where a specific frequency range (here, 83 kHz to 93 kHz) is selected for fitting and a, b, f_0 and Δf are fitting parameters. The central frequency f_0 and the spectrum width Δf are taken as f_{RSAE} and its errorbar respectively. For the present example, the reduction of f_{RSAE} due to ELM is larger than 2 kHz. From the theoretic prediction of f_{RSAE} as in formula (1), f_{RSAE} can be influenced by density, temperature, q_{min} and also plasma rotation. Since the density is reduced by ELM as shown in figure 9(c) and f_{RSAE} is expected to increase, the observed decrease of f_{RSAE} is not due to density reduction. The temperature effect on f_{RSAE} is mainly through the geodesic acoustic term, ω_G. It will be shown below that the temperature effect can also be excluded in present experiment. A $n = 1$ beta-induced Alfvén eigenmode (BAE) is observed on magnetic fluctuation from 3.7 s to 4 s for the shot #71326, as shown in figure 10. It can also be observed in N_{el6} signal, indicating a core-localized mode. The BAE frequency is predicted to be the same as the geodesic acoustic frequency. Figure 10(a) shows that the estimated $n = 1$ BAE frequency around the inner $q = 2$ surface ($\rho = 0.2$) by considering the toroidal rotation, i.e. $f_{BAE} = (\omega_G + n^* V_t/R)/2\pi$, is consistent with the experimental observation. Figure 10(b) shows the time evolution of f_{BAE} of the $n = 1$ BAE in experiment and

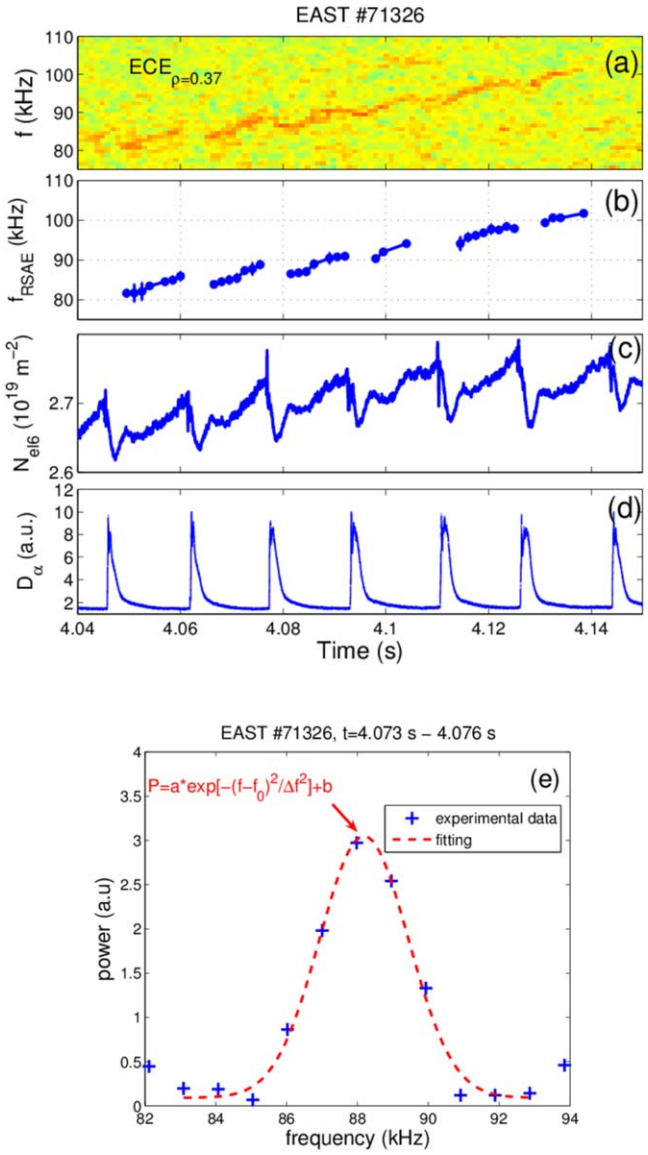

Figure 9. (a) Spectrogram of ECE channel at $\rho = 0.37$, (b) time evolution of RSAE frequency (f_{RSAE}), (c) N_{el6} signal, (d) D_α signal and (e) an example of Gaussian fitting for power spectrum.

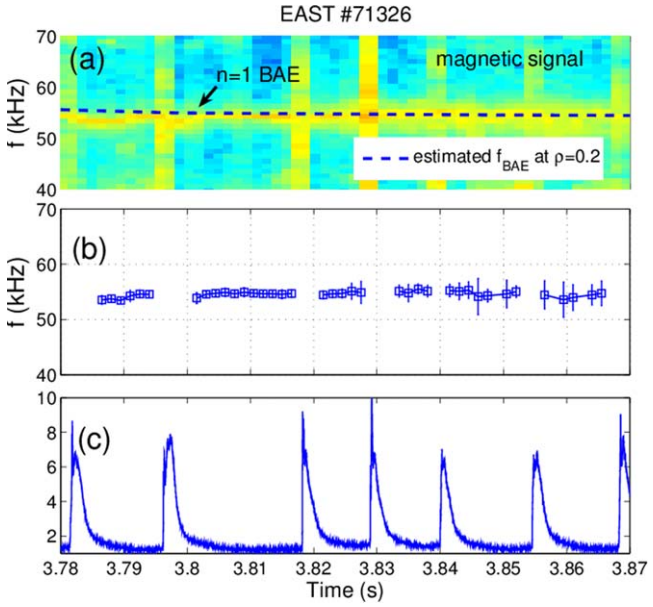

Figure 10. (a) Spectrogram of magnetic signal measured by edge mirnov probe and the estimated $n = 1$ BAE frequency at $\rho = 0.2$, (b) time evolution of $n = 1$ BAE frequency in experiment and (c) D_α signal.

the reduction of f_{BAE} due to ELM is less than 1 kHz. Therefore, the temperature reduction can not solely explain the f_{RSAE} decrease during ELM event. Presently, time definition of rotation measurement is not enough to distinguish ELM event and toroidal mode number of RSAE cannot be determined due to very week magnetic signal on mirnov probe. It is not known whether f_{RSAE} reduction during ELM can be attributed to rotation decrease. Another possibility for this phenomena is that q_{min} is increased, i.e. a broadening of current profile, during ELM event. If this is right, it means that repetitive ELM event in the plasma with RSAE can delay the current diffusion and this would be important for stable and long pulse plasma operation. It is noted that a rapid current profile broadening has been observed due to a coupling between ELM and tearing mode on DIII-D and is beneficial for the maintenance of safety factor above unity in hybrid scenario [38]. The interaction between RSAE and ELM is deserved for study in future.

4. Summary and outlook

We have presented the first observation of the reverse-sheared Alfvén eigenmodes (RSAEs) on EAST tokamak. These modes were observed in different diagnostics, including core channels of interferometer and ECE diagnostics and also edge magnetic probes. Typical feature of these modes is the fast frequency sweeping upward, which cannot be explained by the change of the kinetic profiles and toroidal rotation. Further analysis show that these modes located at a radial range of $\rho = 0.37$–0.46, just around the position of q_{min} at $\rho = 0.4$. Multiple frequency fluctuation modes with frequency sweeping upward, seemingly 'grand cascades', were also clearly observed at $\rho = 0.46$. And it was found that the appearance of these modes was accompanied by the formation of a transient ion ITB. The presented specific example showed that the ITB foot was just at about $\rho = 0.4$, i.e. the position of q_{min}. A modulation of f_{RSAE} by ELM event has been observed. This modulation cannot be explained by density or temperature decrease due to ELM and could be attributed to rotation decrease or q_{min} increase during ELM.

The long pulse high β_{N} operation will be an important task on EAST [29] and how to sustain an optimized q profile is one of the key factors for high performance long pulse operation. It is well known that the Alfvén eigenmodes, e, g, RSAEs and TAEs can be used to constrain the q profile [6] and would be an effective method to accurately determine the

q evolution and important for the successful sustainment of high β_N plasma. On the other hand, present observation in EAST tokamak has showed that these core localized modes are not easily observed by edge magnetic probe, which is the main diagnostics to distinguish these modes in other devices. Therefore, internal measurements of these modes and also the accurate determination of the toroidal and poloidal mode numbers are very important for the application of these modes to diagnose q profile. The reflectometry is a powerful and sensitive diagnostic to measure the density fluctuation and a multichannel poloidal correlation reflectometry has been developed for density fluctuation measurement in the edge on EAST [39]. We have a plan to develop a toroidal/poloidal correlation reflectometry to measure these Alfvén eigenmodes in the plasma core and this diagnostic is expected to detect these modes and determine the toroidal and poloidal mode numbers.

Acknowlegements

This work has been supported by the National Key R&D Program of China (No. 2014GB106004) and National Natural Science Foundation of China (Nos. 11605235, 11675211, 11505221) and Scientific Research Grant of Hefei Science Center of CAS (No. 2015SRG-HSC010).

Appendix. The upper bound of fluctuation poloidal wavenumber measured by diagnostics

For the diagnostics to measure fluctuation using optical method, such as the interferometer or ECE diagnostics in present paper, an upper bound for the poloidal wavenumber (k_θ) of the measurable fluctuation exists. This upper bound is mainly determined by the beam width w. For an Gaussian beam, the beam electric field

$$E \propto \mathrm{e}^{-\frac{y^2}{w^2}} \tag{A.1}$$

where y denotes the coordinate in the poloidal direction. Then for the fluctuation with poloidal wavenumber k_θ, the resultant fluctuation field measured by the diagnostics can be approximately expressed with an integral

$$\begin{aligned} E_\mathrm{f} &\propto \int_{-\infty}^{+\infty} \mathrm{e}^{-\frac{y^2}{w^2}} \mathrm{e}^{\mathrm{i}k_\theta y} \mathrm{d}y \\ &= \sqrt{\pi} w \mathrm{e}^{-\frac{k_\theta^2 w^2}{4}}. \end{aligned} \tag{A.2}$$

For fluctuation analysis, the field amplitude, such as the autopower spectrum shown in figure 3, is usually used. Then from above expression, the fluctuation field amplitude will take

$$S \propto E_\mathrm{f}^2 \propto \mathrm{e}^{-\frac{k_\theta^2 w^2}{2}}. \tag{A.3}$$

It can be seen from this formula that the measured fluctuation field amplitude will be strongly decayed for a large k_θ. Therefore, the upper bound of the measurable k_θ could be determined by setting the S reducing to e^{-2} of the maximum value, i.e.

$$k_\theta \leqslant \frac{2}{w}. \tag{A.4}$$

References

[1] Chen L and Zonca F 2016 *Rev. Mod. Phys.* **88** 015008
[2] Heidbrink W W 2008 *Phys. Plasmas* **15** 055501
[3] ITER Physics Expert Group on Energetic Particles 1999 Heating and current drive and ITER physics basis editors *Nucl. Fusion* **39** 2471
[4] Fasoli A *et al* 2007 *Nucl. Fusion* **47** S264
[5] Breizman B N and Sharapov E 2011 *Plasma Phys. Control. Fusion* **53** 054001
[6] Sharapov E *et al* 2001 *Phys. Lett.* A **289** 127
[7] Fasoli A *et al* 2002 *Plasma Phys. Control. Fusion* **44** B159
[8] Kusama Y *et al* 1998 *Nucl. Fusion* **38** 1215
[9] Kimura H *et al* 1998 *Nucl. Fusion* **38** 1303
[10] Snipes J A *et al* 2000 *Plasma Phys. Control. Fusion* **42** 381
[12] Nazikian R *et al* 2003 *Phys. Rev. Lett.* **91** 125003
[11] Berk H L *et al* 2001 *Phys. Rev. Lett.* **87** 185002
[13] Van Zeeland M A *et al* 2005 *Plasma Phys. Control. Fusion* **47** L31
[14] Fredrickson E D *et al* 2007 *Phys. Plasmas* **14** 102510
[15] Gryaznevich M P *et al* 2008 *Nucl. Fusion* **48** 084003
[16] da Graça S *et al* 2012 *Plasma Phys. Control. Fusion* **54** 095014
[17] Toi K *et al* 2010 *Phys. Rev. Lett.* **105** 145003
[18] Edlund E M *et al* 2009 *Phys. Rev. Lett.* **102** 165003
[19] Sandquist P *et al* 2007 *Phys. Plasmas* **14** 122506
[20] Chen W *et al* 2014 *Nucl. Fusion* **54** 104002
[21] Sharapov S E *et al* 2006 *Nucl. Fusion* **46** S868
[22] Austin M E *et al* 2006 *Phys. Plasmas* **13** 082502
[23] Greenfield C M *et al* 1999 *Nucl. Fusion* **39** 1723
[24] Koide Y *et al* 1994 *Phys. Rev. Lett.* **72** 3662
[25] de Baar M R *et al* 1999 *Phys. Plasmas* **6** 4645
[26] Bell M *et al* 1999 *Plasma Phys. Control. Fusion* **41** A719
[27] Joffrin E *et al* 2002 *Plasma Phys. Control. Fusion* **44** 1739
[28] Joffrin E *et al* 2003 *Nucl. Fusion* **43** 1167
[29] Gao X *et al* 2017 *Nucl Fusion* **57** 056021
[30] Liu F *et al* 2015 *Nucl. Fusion* **55** 123022
[31] Hu C *et al* 2015 *Plasma Sci. Technol.* **17** 1
[32] Liu H Q *et al* 2014 *Rev. Sci. Instrum.* **85** 11D405
[33] Qian J *et al* 2017 *Nucl. Fusion* **57** 036008
[34] Han X *et al* 2014 *Rev. Sci. Instrm.* **85** 073506
[35] Li Y *et al* 2014 *Rev. Sci. Instrm.* **85** 11E428
[36] Lee J *et al* 2014 *Rev. Sci. Instrum.* **85** 063505
[37] Kramer G J *et al* 2006 *Phys. Plasmas* **13** 056104
[38] Petty C C *et al* 2009 *Phys. Rev. Lett.* **102** 045005
[39] Qu H *et al* 2016 *Rev. Sci. Instrm.* **87** 11E707